Online Submissions: wjg.wjgnet.com
www.wjgnet.com
wjg@wjgnet.com

World J Gastroenterol 2007 November 21; 13(43): 5699-5706
World Journal of Gastroenterology ISSN 1007-9327

Characteristics and pathological mechanism on magnetic resonance diffusion-weighted imaging after chemoembolization in rabbit liver VX-2 tumor model

You-Hong Yuan, En-Hua Xiao, Jian-Bin Liu, Zhong He, Ke Jin, Cong Ma, Jun Xiang, Jian-Hua Xiao, Wei-Jian Chen

You-Hong Yuan, Jian-Bin Liu, Department of Radiology, Hunan Province People's Hospital, Changsha 410005, Hunan Province, China
En-Hua Xiao, Zhong He, Cong Ma, Jun Xiang, Department of Radiology, the Second Xiang-Ya Hospital, Central South University, Changsha 410005, Hunan Province, China
Ke Jin, Wei-Jian Chen, Department of Pathology, Hunan Province Children's Hospital, Changsha 410005, Hunan Province, China
Jian-Hua Xiao, Department of Epidemiology, Center for Disease Control of Hunan Province, Changsha 410005, Hunan Province, China
Supported by the National Natural Science Foundation of China, No. 30070235, 30470508
Correspondence to: Dr. You-Hong Yuan, Department of Radiology, Hunan Province People's Hospital, Changsha 410005, Hunan Province, China. heyuanyouhong@yahoo.com.cn
Telephone: +86-731-2278047 Fax: +86-731-2278011
Received: June 5, 2007 Revised: August 17, 2007

Abstract

AIM: To investigate dynamic characteristics and pathological mechanism of signal in rabbit VX-2 tumor model on diffusion-weighted imaging (DWI) after chemoembolization.

METHODS: Forty New Zealand rabbits were included in the study and forty-seven rabbit VX-2 tumor models were raised by implanting directly and intrahepatically after abdominal cavity opened. Forty VX-2 tumor models from them were divided into four groups. DWI was performed periodically and respectively for each group after chemoembolization. All VX-2 tumor samples of each group were studied by pathology. The distinction of VX-2 tumors on DWI was assessed by their apparent diffusion coefficient (ADC) values. The statistical significance between different time groups, different area groups or different b-value groups was calculated by using SPSS12.0 software.

RESULTS: Under b-value of 100 s/mm^2, ADC values were lowest at 16 h after chemoembolization in area of VX-2 tumor periphery, central, and normal liver parenchyma around tumor, but turned to increase with further elongation of chemoembolization treatment. The distinction of ADC between different time groups was significant respectively (F = 7.325, P < 0.001; F = 2.496, P < 0.048; F = 6.856, P < 0.001). Cellular edema in the area of VX-2 tumor periphery or normal liver parenchyma around tumor, increased quickly in sixteen h after chemoembolization but, from the 16th h to the 48th h, cellular edema in the area of normal liver parenchyma around tumor decreased gradually and that in the area of VX-2 tumor periphery decreased lightly at, and then increased continually. After chemoembolization, Cellular necrosis in the area of VX-2 tumor periphery was more significantly high than that before chemoembolization. The areas of dead cells in VX-2 tumors manifested low signal and high ADC value, while the areas of viable cells manifested high signal and low ADC value.

CONCLUSION: DWI is able to detect and differentiate tumor necrotic areas from viable cellular areas before and after chemoembolization. ADC of normal liver parenchyma and VX-2 tumor are influenced by intracellular edema, tissue cellular death and microcirculation disturbance after chemoembolization.

Key words: Liver; VX-2 tumor; Diffusion-weighted imaging; Apparent diffusion coefficient; Chemoembolization

Yuan YH, Xiao EH, Liu JB, He Z, Jin K, Ma C, Xiang J, Xiao JH, Chen WJ. Characteristics and pathological mechanisms on magnetic resonance diffusion-weighted imaging after chemoembolization in rabbit liver VX-2 tumor model. *World J Gastroenterol* 2007; 13(43): 5699-5706

http://www.wjgnet.com/1007-9327/13/5699

INTRODUCTION

Transcatheter arterial chemoembolization (TACE) is a kind of classic interventional therapy and it is commonly performed to treat the unresectable hepatocellular carcinoma and secondary liver cancers. The major goal of chemoembolization is to destroy the tumor. It is very important to evaluate obviously progression of hepatic tumors and differentiate accurately the areas and degrees of necrotic tumor from that of viable tumor before and after chemoembolization.

As reported, ultrasound (US), digital subtraction

angiography (DSA), computed tomography (CT) and magnetic resonance imaging (MRI) are usually used to diagnose and evaluate the progression of hepatic tumor but they have their respective defects. US is able to comprehend the size, blood provision and liquefied or cystic areas of tumor but it can not differentiate necrotic tumor from viable tumor[1,2]. DSA can infer necrotic tumor and viable tumor from the degree of tumor stain. CT can manifest the areas of iodized oil and necrotic or viable tumor but, because density of iodized oil is very high on CT, some areas of necrotic or viable tumor are easily covered before and after chemoembolization[3-5]. MRI is not affected by high density of iodized oil and it is more valuable than US and CT in evaluating the progression of the tumor and in differentiating necrotic from viable tumor. The signals of coagulative necrotic areas of tumor are low on T1- and T2-weighted imaging after chemoembolization and there are no enhanced in MR enhancement scanning[6-11].

Diffusion-weighted imaging is a kind of new functional imaging technology having been developed in recent years and it is the only one method which is able to reflect non-woundingly water molecular diffusion *in vivo*. It has been generally accepted that it is valuable in diagnosing qualitatively and quantitatively cerebral ischemia in hyper-inchoate period[12-14] and, at the same time, many studies of hepatic pathological changes on DWI have been reported[15-17]. ADC values of benign lesions, such as hepatic cysts and hemangiomas, were higher than those of malignant lesions, such as hepatocellular carcinomas and metastases on DWI, as reported by Ichikawa *et al*[15,16], Yamashita *et al*[17], Taouli *et al*[18], Sun *et al*[19]. Colagrande *et al*[20], indicating that the signals of tumor coagulative necrotic areas were lower in comparison with those of tumor viable areas. Kamel *et al*[21] confirmed, in their clinical investigation of 8 case of hepatocellular carcinomas, by image-pathology, that ADC would become high directly with the degree of tumor cellular necrosis increasing and that the signals of 6 tumors were higher than those of normal parenchyma on DWI. Geschwind *et al*[22] demonstrated that the signals of VX-2 tumor necrotic areas were low and that ADC in the area of tumor necrosis were significantly greater than those in the area of viable tumor after chemoembolization.

As indicated by findings of above preliminary experiments, DWI, especially ADC, has potential values in reflecting characteristics of liver pathological changes and of differentiation to benign tumor from malignant one.

There has been no dynamically and image-pathologically investigated report on the characteristics of hepatocellular carcinomas on DWI after chemoembolization. The purpose of our experiment is to investigate dynamic characteristics and pathological mechanism of signal with DWI in rabbit VX-2 tumor model after chemoembolization, which is the most valuable animal model of hepatocellular carcinoma for imaging investigations. Moreover the aim is to evaluate the contribution of DWI in differentiating of tumor viable cells to necrotic ones.

MATERIALS AND METHODS

Animals and establishment of VX-2 tumor model

Animal studies were carried out under the supervision of a veterinarian according to the guidelines on the Use of Laboratory Animals of the Ministry of Public Health of China. All animals were provided by the Laboratory Animal Center of the Second Xiangya Hospital and all protocols were approved by the Animal Use and Care Committee of the Second Xiangya Hospital.

Forty New Zealand rabbits were included in the study. Twenty-two were male rabbits and eighteen were female, weighed 1.7 to 2.5 kg, aged 5 to 6 mo. All of them were healthy. Forty-seven rabbit VX-2 tumor models were raised by implanting the tumor directly and intrahepatically after the abdominal cavity was opened. The VX-2 tumor strain of rabbit was provided by the Fourth Military Medical University.

Forty VX-2 tumor models were layered and randomly chosen from forty-seven VX-2 tumor models and were divided into four groups, including control group (non-interventional group, namely group A) and investigation group (at the 16th h after chemoembolization, at the 32nd h after chemoembolization, at the 48th h after chemoembolization, namely group B, C, and D, respectively). Otherwise, ten cases were randomly chosen from all data were carried out by DWI for all rabbits of group B, C and D at 6th h after chemoembolization and the data was put into group of the 6th h after chemoembolization, as one of investigation groups, namely E group.

Chemoembolization protocol

After DWI at the 21st d after implantation, trans-hepaticartery catheterization chemoembolization was directly and respectively carried out for all rabbits of B, C and D group in the Animal Operating Room of the Second Xiangya Hospital.

First, once rabbits were anesthetized by injecting 3% soluble pentobarbitone and the skin of abdomen was disinfected, then we exposed organs of the hepatic hilar region by incising the skin and vagina musculi recti abdominis. Arteria coeliaca, arteria hepatica communis, arteria hepatica propria, arteria gastroduodenalis, portal vein *etc* were recognized. Second, we drew off arteria gastroduodenalis, we occluded its distalpart and dropped a little attenuated aethocaine on it. Third, we punctured the arteria gastroduodenalis and put plastic transfixion pins or scalp acupunctures into it; the top of transfixion pins were put in arteria hepatica propria. Fourth, we fixed the microtubular or transfixion pins and then infused iodized oil (0.3 mL/kg) and pharmorubicin (2 mg/kg) into arteria hepatica. At last, abdominal membrane, musculature and cutaneous were sutured layer by layer after the liver and other organs in abdominal cavity stopped bleeding.

Magnetic resonance imaging protocol

After animals were anesthetized by injecting 3% soluble pentobarbitone into auriborder vein at a dose of 1 mL/kg or at different doses based on different animal status to make sure that the breathing of animals was slow and stable, DWI(axial) was carried respectively and periodically out a 1.5-Tesla Signa Twinspeed MR scanner (General Electron Medical Systems, USA) using a small diameter cylindrical brain radiofrequency coil before chemoembolization and at the 6th h, the 16th h, the 32nd

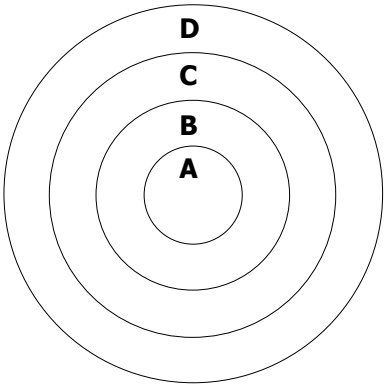

Figure 1 **A**: The area of VX-2 tumor center; **B**: The area of VX-2 tumor periphery; **C**: The area of VX-2 tumor outer layer; **D**: The normal liver parenchyma area around tumor when the values of ADC and signals were measured on DWI and samples were investigated pathologically.

h and the 48th h after chemoembolization. The scanning parameters of DWI included spin echo echoplanar imaging (SE-EPI) series, b-value 100 and 300 s/mm^2, repetition time (TR) 6000 ms, echo time (TE) 45 ms, 20 cm × 15 cm field of view (FOV), 8 number of excitations (NEX), 2 mm thickness layer, 0.5 mm Space, 128 × 128 matrix, *etc*.

ADC values and signal values in the area of VX-2 tumor periphery, in the VX-2 tumor center and in the normal liver parenchyma around tumor (Figure 1) were obtained by using Function Software in GE workstation. Three different regions of interest (ROIs) (50 mm^2 each area) were chosen in the area of normal liver parenchyma (area D in Figure 1) and we measured their ADC values and signal values. The average value of above was considered as the ADC value or the signal value of normal liver parenchyma around tumor. The thickness of area A and B in Figure 1 was respectively two fifth diameter of VX-2 tumor. By the same methods, the average value of three different ROIs ADC values or signal values in area B was considered as the ADC value or the signal value of VX-2 tumor periphery area; ADC value or signal value of area A was its ADC value or signal value of VX-2 tumor center area. All measurements were finished cooperatively by two senior attending physicians or associate professors.

Pathology protocol

All of the rabbits in each group were euthanized by injecting an overdose of 3% soluble pentobarbitone into auriborder vein when DWI was respectively carried out before chemoembolization, and after the 16 h, the 32 h and 48 from chemoembolization. We got layer by layer VX-2 samples under the condition of asepsis (Figure 1) and made them fixed in the formaldehyde solution for 24 h before being embedded in mineral wax. Each VX-2 tumor was divided into the outer layer area, the periphery area and the center area (Figure 1) so that samples included four parts: VX-2 tumor center area, VX-2 tumor periphery area, VX-2 tumor outer layer area and normal liver parenchyma around tumor.

All samples were investigated respectively under 100 × and 400 × microscope and the emphases were on investigating cellular edema in the VX-2 tumor and normal liver parenchyma around tumor.

Edema index was used to estimate the degree of cellular edema, which was the contrast of edema cell number to total cells under microscope. Manifestations of edema cells under microscope included cell body increasing, unclear cellular membrane and intracytoplasm vacuolar or ballooning degeneration; the latter was the most important manifestation of edema cell. Two campus visualises under 400 × microscope were obtained randomly in the zone of non-necrosis. The number of edema cells and total cell number were counted by two external doctors not from our study team with double blind method. Otherwise, we investigated specially the degree of tumor cellular necrosis and the abnormity of cell membrane. Statistical analysis based on apparent diffusion coefficient (ADC) value of ROIs and edema index, the distinction between different area groups, different time groups and different b-value groups was respectively estimated. The statistical significance was calculated by analysis of variance (ANOVA) or analysis of non-parameter by using SPSS software (version 12.0; SPSS, Tokyo, Japan)

RESULTS

Image manifestations of hepatic VX-2 tumor before and after chemoembolization

ADC values and signal values of VX-2 tumors were shown in Table 1 and Figures 2-5.

The distinction between ADC in the area of VX-2 tumor periphery, tumor center or normal parenchyma around tumor was respectively significant ($F = 14.366$, $P < 0.001$; $F = 4.674$, $P = 0.033$; $F = 23.054$, $P < 0.001$) with b-value 100 s/mm^2 and with b-value is 300 s/mm^2 was respectively significant ($F = 14.366$, $P < 0.001$; $F = 4.674$, $P = 0.033$; $F = 23.054$, $P < 0.001$). Signals in the area of VX-2 tumor periphery, tumor center and normal parenchyma around tumor b-value was 100 s/mm^2 were higher than with b-value was 300 s/mm^2 ($F = 112.874$, $P < 0.001$; $F = 83.455$, $P < 0.001$; $F = 135.455$, $P < 0.001$).

When b-value was 100 s/mm^2, the distinction of ADC in the area of VX-2 tumor periphery, tumor center and normal parenchyma around tumor among group A, B, C, D and E was respectively significant($F = 7.325$, $P < 0.001$; $F = 2.496$, $P = 0.048$; $F = 6.856$, $P < 0.001$). The distinction of signal in the area of VX-2 tumor periphery among group A, B, C, D and E was significant ($F = 3.005$, $P < 0.05$) but that in the area of VX-2 tumor center and normal parenchyma around tumor was not significant ($F = 1.399$, $P > 0.05$; $F = 2.146$, $P > 0.05$).

Manifestations of VX-2 tumor pathology

Observed by the naked eye, most surfaces of normal hepatic parenchyma around VX-2 tumor were paler in investigation group than those in control group and there was embolization of unequal areas but well-circumscribed. The tumors were hard and there was clear demarcation. The cavities of unequal size were found in the area of VX-2 tumors because kermesinus liquid had run off after the tumors werfae cut open.

Under microscope, some edema cells containing ballooning degeneration were observed in the area of normal parenchyma around VX-2 tumor. Inequality

Table 1 ADC values of tumor and normal parenchyma after Chemoembolization

Group	VX-2 tumor periphery areas		VX-2 tumor center areas		Hepatic normal parenchyma	
	b = 100	b = 300	b = 100	b = 300	b = 100	b = 300
Control	1.71 ± 0.27	1.48 ± 0.23	1.77 ± 0.36	1.55 ± 0.30	2.71 ± 0.42	2.30 ± 0.40
6 h	1.56 ± 0.40	1.36 ± 0.18	1.97 ± 0.49	1.79 ± 0.37	2.44 ± 0.53	1.87 ± 0.31
16 h	1.24 ± 0.22	1.12 ± 0.20	1.56 ± 0.40	1.69 ± 0.35	2.10 ± 0.54	1.65 ± 0.37
32 h	1.48 ± 0.37	1.23 ± 0.16	1.99 ± 0.32	1.66 ± 0.31	2.10 ± 0.49	1.97 ± 0.29
48 h	1.57 ± 0.23	1.40 ± 0.18	2.04 ± 0.54	1.82 ± 0.27	2.43 ± 0.33	2.06 ± 0.23
Total	1.51 ± 0.33	1.32 ± 0.23	1.87 ± 0.45	1.70 ± 0.32	2.36 ± 0.51	1.97 ± 0.38

Data are expressed as mean ± SD × 10^{-3} mm^2/s; ADC: Apparent diffusion coefficient.

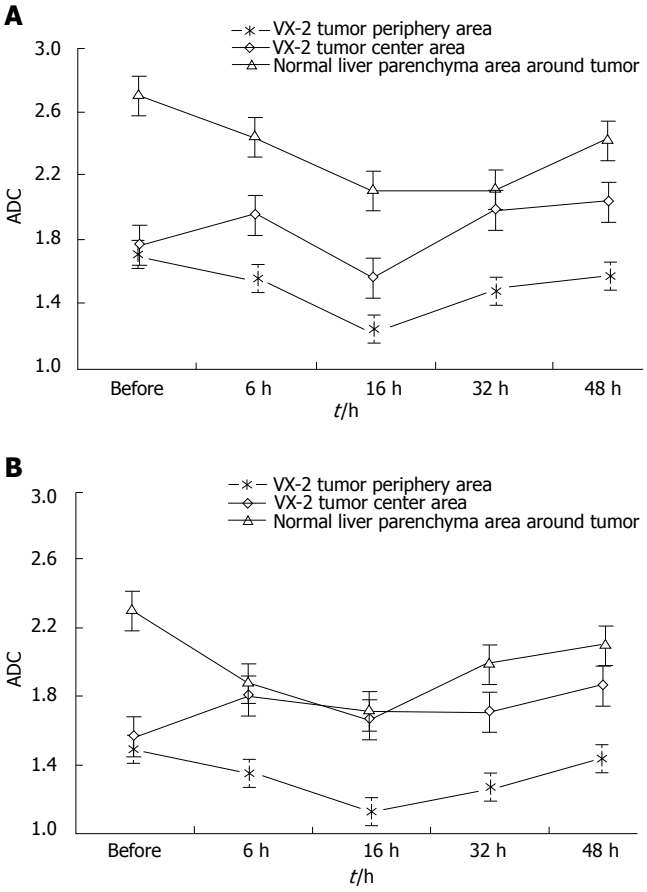

Figure 2 ADC values of different areas on DWI after chemoembolization. **A**: B-value was 100 s/mm^2; **B**: B-value was 300 s/mm^2.

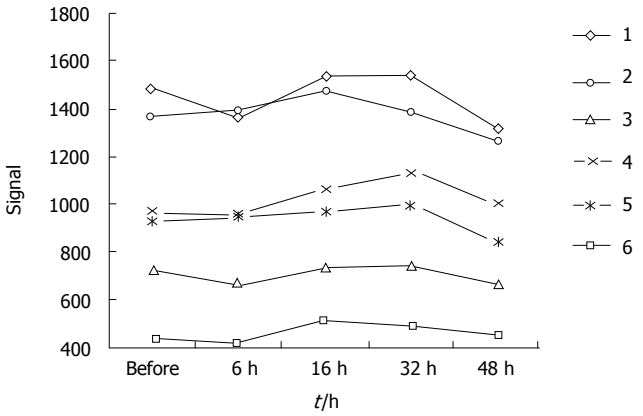

Figure 3 Signal values on DWI when area and b-value was different after chemoembolization. Areas: 1-signal of VX-2 tumor periphery area when b-value was 100 s/mm^2; 2-signal of VX-2 tumor center area when b-value was 100 s/mm^2; 3-signal of the normal liver parenchyma area around tumor when b-value was 100 s/mm^2; 4-signal of VX-2 tumor periphery area when b-value was 300 s/mm^2; 5-signal of VX-2 tumor center area when b-value was 300 s/mm^2; 6-signal of the normal liver parenchyma area around tumor when b-value was 300 s/mm^2.

of size, round or ellipse or strip tumor nests could be observed in different areas of VX-2 tumor. The degree of cell edema and necrosis were more obvious in group B,C and D (after chemoembolization) than group A (before chemoembolization), the necrotic areas were more in the area of VX-2 tumor center than those in the area of tumor periphery or tumor outer layer, and most areas of tumor center were necrotic in some VX-2 tumors.

Edema cells showed their volume increased obviously, kytoplasm dyeing thinly and obvious ballooning degeneration (Figure 6 and 7). Dynamical information of cellular edema and necrosis were counted in Tables 2 and 3.

DISCUSSION

The signal and ADC characteristics of many hepatic pathological changes on DWI have been reported in recent years[23-26]. DWI has significant and potential clinical application values in detecting, diagnosing and differentiating tumors earlier. From what has been determined when DWI was investigated by Yuan *et al* in rabbit liver VX-2 tumor model, VX-2 tumor is a solid tumor and its body mainly consists of tumor nests and other cells so that its water molecule diffusion motion is obviously restricted, the signal of them is significantly high and ADC is significantly low.

The signals in VX-2 tumors were higher than those in the area of normal parenchyma around tumor while ADC values were lower than those in the area of normal parenchyma after chemoembolization, and the tendency of the signal and ADC in VX-2 tumors and in the area of normal parenchyma was basically the same. The signals in VX-2 tumors were uneven, the signals in the area of tumor center were lower than that in the area of tumor periphery, while those in the 48 h after chemoembolization were lower than that before chemoembolization. The areas of low signal and high signal were observed in VX-2 tumor and ADC of them was higher than that in the equal signal area of VX-2 tumor or in the area of normal parenchyma. Accordingly with pathology, the areas of low signal in VX-2 tumor were coagulation necrosis, those of high signal were liquid or cystic tissue,

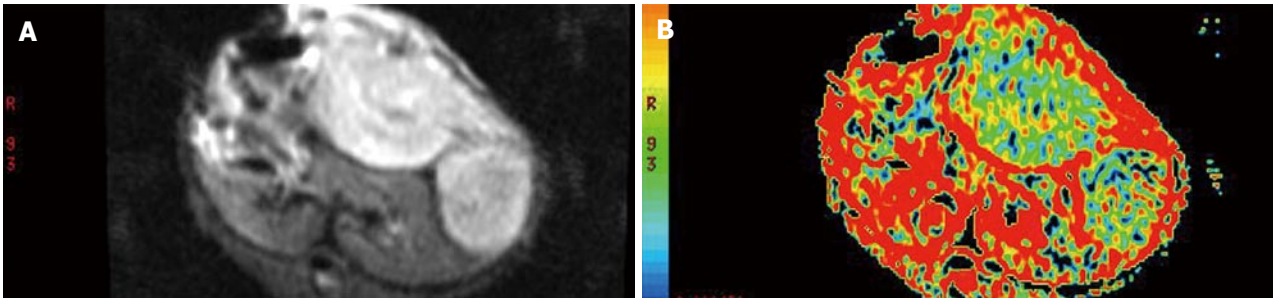

Figure 4 Image manifestations of hepatic VX-2 tumor on DWI and ADC map when b-value was 100 s/mm^2 at 6 h after chemoembolization **A**: High signal and distinct margin of VX-2 tumor on DWI; **B**: Low signal of it on the ADC map.

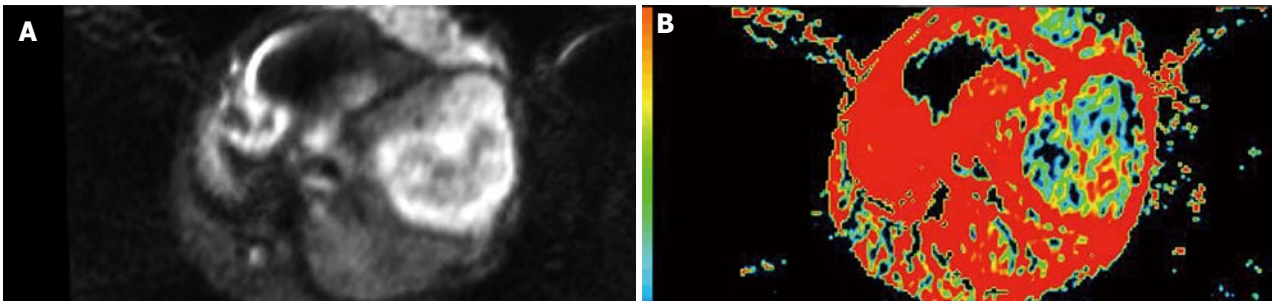

Figure 5 Image manifestations of hepatic VX-2 tumor on DWI and ADC map when b-value was 100 s/mm^2 at 48 h after chemoembolization **A**: High and uneven signal and distinct margin of VX-2 tumor on DWI; **B**: Low and uneven signal of it on the ADC map.

and other areas except low signal and high signal areas in the lump were viable tumor cells. Moreover, necrotic areas in VX-2 tumors after chemoembolization were more than those before chemoembolization. When coagulation necrosises/necroses takes place in the tumor because of insufficient blood provision, cellular membrane will break and the limitation of water molecular motion in the tumor decreases greatly so that the signals is reduced while ADC values are upgraded. After coagulation necroses have been liquefied or become cystic, cell lysis and leakier cell membranes can no longer compartmentalize water molecules and allow free diffusion to take place so that ADC values increase greatly. Nyway the signals of above mentioned liquefied or cystic areas are higher than those of coagulative necrosis areas, even viable tumor areas or normalparenchyma. It can be explained by the presence of greater amounts of extracellular water molecules within the necrotic region which is a kind of long T2-value contribution constitution and the b-value is 100 or 300 s/mm^2, a small b-value, in diffusion-weighted imaging scanning so that the signals of above are affected significantly by "shine-through".

At 6 h after chemoembolization, the signals in the area of tumor centers decreased slightly while ADC increased slightly, the signals in the area of tumor periphery and normal parenchyma increased significantly while ADC decreased at different degrees. However, pathology demonstrated that the degree of cellular necrosis in the area of normal parenchyma before chemoembolization was the same of that after chemoembolization while in the area of tumor periphery areas before chemoembolization was much more than after chemoembolization.

Accordingly with what discussed above, the signal increasing and ADC decreasing cannot completely be explained by tumor cellular necrosis after chemoembolization. The dynamic mechanisms of water molecular diffusion decreasing and the signal increasing while ADC values decreasing after cerebral infarction have been investigated by many investigators in recent years, and it is not completely comprehended yet, but most of them demonstrated it was connected with cytotoxic edema, microcirculation disturbance, temperature or abnormality of cellular membrane permeability, *etc*[27-31]. A series of clinical and animal experimental investigations by Xie *et al*[28], Han *et al*[29] and Marks *et al*[30] have demonstrated that the cytotoxic edema after embolization had significant influences on the change of water molecules diffusion. Because of dysfunctional Na-K pump due to early hypoxia after embolization, the density of intra-cellular electrolyte increases and then also water molecules of intra-cells increase significantly, while extra-cell water molecules decrease significantly, so that ADC starts decreasing while the signal starts increasing. When intracellular edema reaches to the biggest degree, ADC of constitution will decrease to the lowest and it will maintain at a low degree if intracellular edema maintains or if there are constitution edema originating from the blood vessel. ADC of constitution will start increasing after cellular membrane has been broken and cells have dissolved; it will reach the biggest when constitution has been liquefied and become cystic.

After chemoembolization, ADC in the area of VX-2 tumor periphery and normal parenchyma decreased quickly wuth ther bottom at biggest in the 16th h and

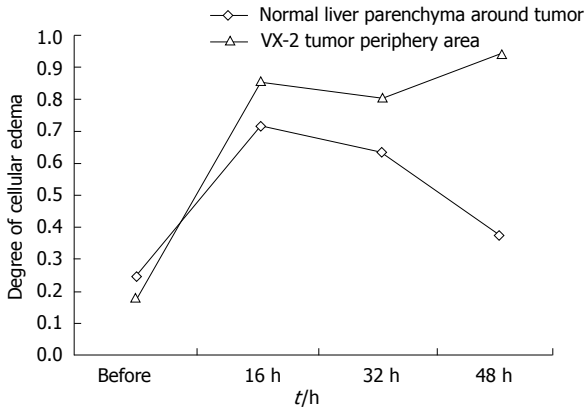

Figure 6 Cellular edema of different areas after chemoembolization.

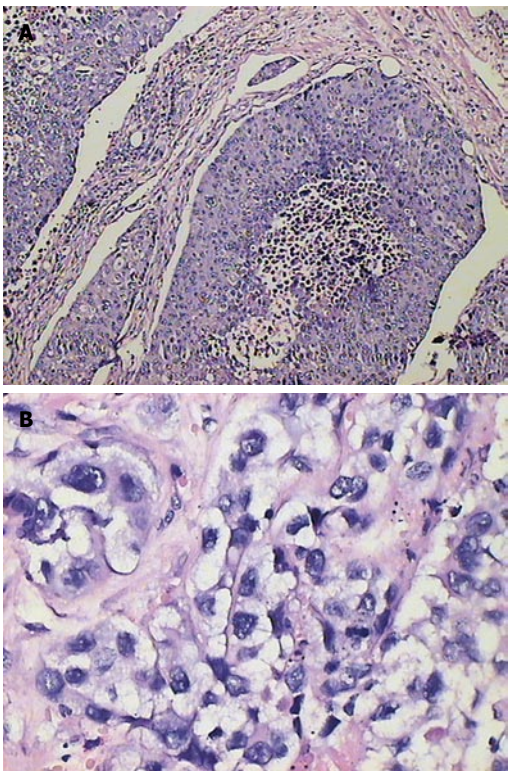

Figure 7 **A**: Cell nest of VX-2 tumor and wide zone of necrosis in the tumor(x 100) and **B**: cellular edema in the VX-2 tumor (x 400).

then increased gradually but they were significantly lower in the 48th h after chemoembolization than those before chemoembolization. Pathology demonstrated the degree of cellular edema in the area of VX-2 tumor and normal parenchyma were significant higher after chemoembolization than before chemoembolization and it reaching a peak at 16th h after chemoembolization and then decreased gradually. The signal and ADC changes in the area of VX-2 tumor and normal parenchyma were significantly relative to cellular edema. The function of Na-K pump decreases or misses because of ischemia and hypoxia from chemoembolization and toxic action from chemotherapeutic drug; the degree of intra-cell edema also increases significantly after chemoembolization so that ADC starts decreasing. With intracellular edema lessening

Table 2 Dynamic information of cellular edema after chemoembolization (%) (mean ± SD)

	Control	16 h	32 h	48 h
Normal parenchyma	24.90 ± 11.69	72.12 ± 34.48	63.89 ± 29.87	38.00 ± 24.57
Tumor periphery areas	18.16 ± 10.35	86.06 ± 16.01	81.18 ± 20.03	96.66 ± 4.76

Table 3 Manifestations of VX-2 tumor pathology after chemoembolization

	Cellular membrane		Cellular necrosis			
	0	1	0	1	2	3
Normal parenchyma (Control)	8	2	7	3		
Tumor periphery areas (Control)	10				9	1
Normal parenchyma (16 h)	7	3	7	1	2	
Tumor periphery areas (16 h)	10			2	4	4
Normal parenchyma (32 h)	7	3	7	1	2	
Tumor periphery areas (32 h)	10				3	7
Normal parenchyma (48 h)	6	4	8	2		
Tumor periphery areas (48 h)	10				4	6

Cellular membrane: 0-clear and complete; 1-unclear and non-complete. Cellular necrosis: 0-cellular structure existing and cellular membrane complete; 1-many cells dissolving and cellular membrane disappearing; 2-minute cellular coagulation necrosis; 3-extensive cellular coagulation necrosis.

or cell breaking, ADC values will increase gradually. The dynamic changes of ADC can reflect the degree of tumor cellular edema and cellular necrosis.

However, after chemoembolization, ADC in the area of VX-2 tumor periphery and normal parenchyma increased gradually but the signals decreased gradually from the 16th h to the 48th h after chemoembolization; the signals were lower in the 48th h than those before chemoembolization. Pathology demonstrated that the degree of cellular edema in the area of normal parenchyma reached a peak in the 16th h and then decreased gradually but that in the area of tumor periphery reached a peak in the 16th h and then increased continually after chemoembolization. The degree of cellular edema in the area of tumor periphery was significantly lower than that in the area of normal parenchyma. Double blood-provision from hepatic artery and portal system plus our protocols of transcatheter hepaticarterial chemoembolization can explain it. Selective catheterization was not carried out in our experiments so that ischemia and hypoxia took place in the VX-2 tumor and normal parenchyma at the same time and ADC decreased because of intracellular edema. The degree of cellular edema in VX-2 tumor was higher than that in the area of normal parenchyma after chemoembolization because 95%-99% blood provision of hepatocellular carcinoma comes from hepatic artery while 70%-75% blood provision of normal parenchyma comes from portal system and others comes from hepatic artery. Blood provision from portal system would recover step by step after chemoembolization so that the degree of cellular edema in the area of normal parenchyma decreased significantly but that in VX-2

tumor increased continually from the 16 h to the 48 h after chemoembolization. Otherwise, as reported by Yang *et al*[31], blood provision decreasing could lead to ADC decreasing and ADC reflected blood provision to a certain degree when b-value was small in diffusion-weighted imaging scanning. Since b-value was small in our scanning, ADC could be affected by blood provision after chemoembolization.

Necrotic tumor manifests low signal and high ADC value, while viable tumor manifests high signal and low ADC value after chemoembolization. DWI has potential ability in detecting and differentiating viable tumor from necrotic tumor and, besides water molecular diffusion, intracellular edema, microcirculation disturbance and tumor necrosis from chemoembolization are significantly relative to ADC changing dynamically.

ACKNOWLEDGMENTS

We thank the staff of the Radiology Department and the Laboratory Animal Center of the Second Xiangya Hospital for their help, especially Ying-Si He.

COMMENTS

Background

Transcatheter arterial chemoembolization (TACE) is a kind of classic interventional therapy and it is commonly performed to treat the unresectable hepatocellular carcinoma and most secondary liver cancers. The major goal of chemoembolization is to destroy the tumor. Ultrasound (US), digital subtraction angiography (DSA), computed tomography (CT) and magnetic resonance imaging (MRI) are usually used to diagnose and to evaluate the progression of hepatic tumor but they have their respective defects. Diffusion-weighted imaging is a kind of new functional imaging technology having been developed in recent years and it is the only one method which is able to reflect non-woundingly water molecular diffusion *in vivo*. Geschwind *et al* demonstrated that the signals of VX-2 tumor necrotic areas were low and ADC of them were significantly greater in the area of tumor necrosis than those in the area of viable tumor after chemoembolization. Therefore, we believe that DWI, especially ADC, has potential values in reflecting characteristics of liver pathological changes and differentiating benign tumor from malignant one.

Research frontiers

Many studies of hepatic pathological changes on DWI have been reported. ADC values of benign lesions, such as hepatic cysts and hemangiomas, were higher than those of malignant lesions, such as hepatocellular carcinomas and metastases on DWI and many studies also indicated that the signals of tumor coagulative necrotic areas were lower in comparison with that of tumor viable areas. There has been no dynamically and image-pathologically investigated report on the characteristics of hepatocellular carcinomas on DWI after chemoem-bolization.

Innovations and breakthroughs

Our study clearly showed that necrotic tumor manifested low signal and high ADC value while viable tumor manifested high signal and low ADC value after chemoembolization. DWI would have potential ability in detecting and differentiating viable tumor from necrotic tumor and, besides water molecular diffusion, intracellular edema, microcirculation disturbance and tumor necrosis from chemoembolization were significantly relative to ADC changing dynamically.

Applications

Physicians can apply this knowledge to evaluate obviously progression of hepatic tumors and differentiate accurately the areas and degrees of necrotic tumor from that of viable tumor before and after chemoembolization.

Peer review

This is an interesting, well designed, and written study on a problem of real clinical significance.

REFERENCES

1 **Morimoto M**, Shirato K, Sugimori K, Kokawa A, Tomita N, Saito T, Imada T, Tanaka N, Nozawa A, Numata K, Tanaka K. Contrast-enhanced harmonic gray-scale sonographic-histologic correlation of the therapeutic effects of transcatheter arterial chemoembolization in patients with hepatocellular carcinoma. *AJR Am J Roentgenol* 2003; **181**: 65-69

2 **Kubota K**, Hisa N, Nishikawa T, Fujiwara Y, Murata Y, Itoh S, Yoshida D, Yoshida S. Evaluation of hepatocellular carcinoma after treatment with transcatheter arterial chemoembolization: comparison of Lipiodol-CT, power Doppler sonography, and dynamic MRI. *Abdom Imaging* 2001; **26**: 184-190

3 **Ebied OM**, Federle MP, Carr BI, Pealer KM, Li W, Amesur N, Zajko A. Evaluation of responses to chemoembolization in patients with unresectable hepatocellular carcinoma. *Cancer* 2003; **97**: 1042-1050

4 **Kim HC**, Kim AY, Han JK, Chung JW, Lee JY, Park JH, Choi BI. Hepatic arterial and portal venous phase helical CT in patients treated with transcatheter arterial chemoembolization for hepatocellular carcinoma: added value of unenhanced images. *Radiology* 2002; **225**: 773-780

5 **Shankar S**, vanSonnenberg E, Morrison PR, Tuncali K, Silverman SG. Combined radiofrequency and alcohol injection for percutaneous hepatic tumor ablation. *AJR Am J Roentgenol* 2004; **183**: 1425-1429

6 **Minami Y**, Kudo M, Kawasaki T, Kitano M, Chung H, Maekawa K, Shiozaki H. Transcatheter arterial chemoembolization of hepatocellular carcinoma: usefulness of coded phase-inversion harmonic sonography. *AJR Am J Roentgenol* 2003; **180**: 703-708

7 **Zhang Z**, Wu M, Chen H, Chen D, He J. Percutaneous radiofrequency ablation combined with transcatheter arterial chemoembolization for hepatocellular carcinoma. *Zhonghua Waike Zazhi* 2002; **40**: 826-829

8 **Seki T**, Tamai T, Ikeda K, Imamura M, Nishimura A, Yamashiki N, Nakagawa T, Inoue K. Rapid progression of hepatocellular carcinoma after transcatheter arterial chemoembolization and percutaneous radiofrequency ablation in the primary tumour region. *Eur J Gastroenterol Hepatol* 2001; **13**: 291-294

9 **Chan JH**, Tsui EY, Luk SH, Yuen MK, Cheung YK, Wong KP. Detection of hepatic tumor perfusion following transcatheter arterial chemoembolization with dynamic susceptibility contrast-enhanced echoplanar imaging. *Clin Imaging* 1999; **23**: 190-194

10 **Tsui EY**, Chan JH, Cheung YK, Cheung CC, Tsui WC, Szeto ML, Lau KW, Yuen MK, Luk SH. Evaluation of therapeutic effectiveness of transarterial chemoembolization for hepatocellular carcinoma: correlation of dynamic susceptibility contrast-enhanced echoplanar imaging and hepatic angiography. *Clin Imaging* 2000; **24**: 210-216

11 **Lövblad KO**, Wetzel SG, Somon T, Wilhelm K, Mehdizade A, Kelekis A, El-Koussy M, El-Tatawy S, Bishof M, Schroth G, Perrig S, Lazeyras F, Sztajzel R, Terrier F, Rüfenacht D, Delavelle J. Diffusion-weighted MRI in cortical ischaemia. *Neuroradiology* 2004; **46**: 175-182

12 **Na DG**, Thijs VN, Albers GW, Moseley ME, Marks MP. Diffusion-weighted MR imaging in acute ischemia: value of apparent diffusion coefficient and signal intensity thresholds in predicting tissue at risk and final infarct size. *AJNR Am J Neuroradiol* 2004; **25**: 1331-1336

13 **O'Donnell ME**, Tran L, Lam TI, Liu XB, Anderson SE. Bumetanide inhibition of the blood-brain barrier Na-K-Cl cotransporter reduces edema formation in the rat middle cerebral artery occlusion model of stroke. *J Cereb Blood Flow Metab* 2004; **24**: 1046-1056

14 **Ichikawa T**, Haradome H, Hachiya J, Nitatori T, Araki T. Diffusion-weighted MR imaging with a single-shot echoplanar sequence: detection and characterization of focal hepatic lesions. *AJR Am J Roentgenol* 1998; **170**: 397-402

15 **Ichikawa T**, Haradome H, Hachiya J, Nitatori T, Araki T. Diffusion-weighted MR imaging with single-shot echo-planar imaging in the upper abdomen: preliminary clinical experience in 61 patients. *Abdom Imaging* 1999; **24**: 456-461

16 **Yamashita Y**, Tang Y, Takahashi M. Ultrafast MR imaging of the abdomen: echo planar imaging and diffusion-weighted imaging. *J Magn Reson Imaging* 1998; **8**: 367-374
17 **Taouli B**, Martin AJ, Qayyum A, Merriman RB, Vigneron D, Yeh BM, Coakley FV. Parallel imaging and diffusion tensor imaging for diffusion-weighted MRI of the liver: preliminary experience in healthy volunteers. *AJR Am J Roentgenol* 2004; **183**: 677-680
18 **Sun XJ**, Quan XY, Liang W, Wen ZB, Zeng S, Huang FH, Tang M. Quantitative study of diffusion weighted imaging on magnetic resonance imaging in focal hepatic lesions less than 3 cm. *Zhonghua Zhongliu Zazhi* 2004; **26**: 165-167
19 **Colagrande S**, Politi LS, Messerini L, Mascalchi M, Villari N. Solitary necrotic nodule of the liver: imaging and correlation with pathologic features. *Abdom Imaging* 2003; **28**: 41-44
20 **Kamel IR**, Bluemke DA, Ramsey D, Abusedera M, Torbenson M, Eng J, Szarf G, Geschwind JF. Role of diffusion-weighted imaging in estimating tumor necrosis after chemoembolization of hepatocellular carcinoma. *AJR Am J Roentgenol* 2003; **181**: 708-710
21 **Geschwind JF**, Artemov D, Abraham S, Omdal D, Huncharek MS, McGee C, Arepally A, Lambert D, Venbrux AC, Lund GB. Chemoembolization of liver tumor in a rabbit model: assessment of tumor cell death with diffusion-weighted MR imaging and histologic analysis. *J Vasc Interv Radiol* 2000; **11**: 1245-1255
22 **Somford DM**, Marks MP, Thijs VN, Tong DC. Association of early CT abnormalities, infarct size, and apparent diffusion coefficient reduction in acute ischemic stroke. *AJNR Am J Neuroradiol* 2004; **25**: 933-938
23 **Brugières P**, Thomas P, Maraval A, Hosseini H, Combes C, Chafiq A, Ruel L, Breil S, Peschanski M, Gaston A. Water diffusion compartmentation at high b values in ischemic human brain. *AJNR Am J Neuroradiol* 2004; **25**: 692-698
24 **Mitsias PD,** Ewing JR, Lu M, Khalighi MM, Pasnoor M, Ebadian HB, Zhao Q, Santhakumar S, Jacobs MA, Papamitsakis N, Soltanian-Zadeh H, Hearshen D, Patel SC, Chopp M. Multiparametric iterative self-organizing MR imaging data analysis technique for assessment of tissue viability in acute cerebral ischemia. *AJNR Am J Neuroradiol* 2004; **25**: 1499-1508
25 **Moteki T**, Horikoshi H, Oya N, Aoki J, Endo K. Evaluation of hepatic lesions and hepatic parenchyma using diffusion-weighted reordered turboFLASH magnetic resonance images. *J Magn Reson Imaging* 2002; **15**: 564-572
26 **Wang JL**, Xie JX. Assessment of hemodynamics and pathophysiology of acute cerebral ischemia with MR perfusion-weighted imaging and dynamic diffusion-weighted imaging. *Zhonghua Fangshexue Zazhi* 1998; **32**: 370-374
27 **Xiao XH**, Kong XQ, Jiang Li, Jiang L, Wang YM, Xu HB, Li LY, Tang YF. An experimental study on acute cerebral ischemia and reperfusion with magnetic resonance diffusion weighted imaging. *Zhonghua Fangshexue Zazhi* 1999; **33**: 662-666
28 **Xie JX**, Fu Y, Zhang Y. The change of water cellular diffusion motion and its clinical application. *Beijing Daxue Xuebao* (Yixueban) 2001; **33**:109-112
29 **Han HB**, Xie JX. Application of EPI diffusion- weighted and Gd DTPA2 perfusion imaging in the diagnosis of brain ischemia. *Zhonghua Fangshexue Zazhi* 1998; **32**: 364-369
30 **Marks MP**, de Crespigny A, Lentz D, Enzmann DR, Albers GW, Moseley ME. Acute and chronic stroke: navigated spin-echo diffusion-weighted MR imaging. *Radiology* 1996; **199**: 403-408
31 **Yang ZH**, Xie JX, Zhang YW, HU BF. Study on diffusion-weighted imaging in cirrhotic liver. *Zhongguo Yixue Yingxiang Jishu* 2002; **9**: 907-909

S- Editor Zhu LH **L- Editor** Li M **E- Editor** Yin DH